Asian Journal of Research and Reviews in Physics

Volume 7, Issue 2, Page 1-14, 2023; Article no.AJR2P.98416
ISSN: 2582-5992

Studies on the Optical Dispersion Parameters and Electronic Polarizability of Cadmium Sulphide Thin Film

O. Okorie [a*] and A. D. A. Buba [b]

[a] Department of Theoretical Physics, National Mathematical Centre, 904105 Abuja, Nigeria.
[b] Department of Physics, Faculty of Science, University of Abuja, 900211 Abuja, Nigeria.

Authors' contributions

This work was carried out in collaboration between both authors. Both authors read and approved the final manuscript.

Article Information

DOI: 10.9734/AJR2P/2023/v7i2134

Open Peer Review History:
This journal follows the Advanced Open Peer Review policy. Identity of the Reviewers, Editor(s) and additional Reviewers, peer review comments, different versions of the manuscript, comments of the editors, etc are available here: https://www.sdiarticle5.com/review-history/98416

Original Research Article

Received: 07/02/2023
Accepted: 10/04/2023
Published: 20/04/2023

ABSTRACT

Thin film of Cadmium Sulphide (CdS) was deposited onto a precleaned transparent glass substrate by chemical bath deposition technique from a bath containing Cadmium acetate, ammonium acetate, thiourea and ammonium hydroxide. The deposition time was varied from 10 minutes to 50 minutes at an interval of 20 minutes keeping the bath at a constant temperature of 90℃ using 78HW-1 constant magnetic stirrer. CdS thin film was characterized by UV-Visible spectrophotometer within the wavelength range of 280 nm – 920 nm using Single – Beam Helios Omega UV – VIS spectrophotometer. The optical parameters; extinction coefficient, refractive index and dielectric constant of CdS thin film were analyzed from the absorption spectra and were found to be affected by the deposition time. The optical band gap energy was obtained by Tauc's equation and were found to decrease from 3.78 eV – 3.70 eV as the deposition time increases. The dispersion parameters (dispersion energy E_d, oscillation energy E_o, moment of optical dispersion

**Corresponding author: E-mail: okike_isu@yahoo.com;*

spectra m_{-1} and m_{-3}, static dielectric constant ε_o and static refractive index η_o) were calculated using theoretical Wemple-DiDomenico model. The result show that only E_o and E_d behaved differently but other parameters increase as the deposition time increases. The oscillator strength S_o, oscillator wavelength λ_o, high frequency dielectric constant ε_∞ and high frequency refractive index η_∞ were calculated using single Sellmeier oscillator model. While S_o behaved differently other parameters increase as the deposition time increased. Also, Lattice dielectric constant ε_L, N/m* and plasma resonance frequency ω_p were equally obtained. While ε_L decrease with increase in deposition time, N/m* increase with deposition time. The electronic polarizability α_p of CdS thin film was estimated by Lorenz - Lorentz equation and Clausius Mossotti local field polarizability model. The value is an indication that the films showed good response on the application of photon energy. However, its response reduces as the deposition time increases.

Keywords: Dispersion parameter; Wemple-DiDomenico model; single Sellmeier oscillator model; Clausius-Mossotti local field polarizability; CdS thin film.

1. INTRODUCTION

The properties of Semiconductor materials are very important for determining their applicability in various fields. Moreover, in nanoscale some of the properties have been affected that made it differ from the bulk material especially the bandgap [1–4]. Since it is possible to adjust or tailor their electrical and optical properties especially when physical dimensions are reduced to a few nanometers which these properties depend upon, that makes them useful for application in optoelectronics, nonlinear optics and photoelectrochemical solar cell devices [1,4-6]. "Dispersion parameters can be determined by parameterization of data. This is because these parameters depend on the dielectric functions of films and other corresponding function such as the bandgap, optical dispersion energies (E_o, E_d), dielectric constant $(\varepsilon,)$ ratio between the number of charge carriers and effective mass $\left(\frac{N}{M^*}\right)$ wavelength of the single oscillator λ_o, and plasma frequency ω_p. These parameters, especially the optical constants provide information about the microscopic characteristics of the material" [7].

Chalcogenide semiconductors such as Cadmium Sulphide (CdS) have shown great usefulness and applicability in solar cells and optoelectronics such as linear and nonlinear optics, visible light diodes, and lasers [8,9]. "This is because CdS has wide bandgap, low absorption loss, compact crystallographic cell structure and electronic affinity" [10]. "Moreso, CdS, is most widely used as a window layer in CdTe thin film solar cells and is a buffer layer in Copper Indium and Gallium Selenide (CIGS) thin film solar cells" [11–15].

"Several deposition techniques have been studied and employed in the fabrication of CdS thin films such as spin coating [16], Electro deposition ED [17], physical vapour deposition PVD [18], spray pyrolysis [19-21], Successive ionic layer adsorption and reaction SILAR [22], chemical precipitation [23], Sol - gel deposition [24,25], Thermal evaporation [26,27], and Chemical bath deposition CBD" [2,28-31].

"Among all these techniques for synthesizing CdS, CBD has been adjudged to be the simplest, does not require sophisticated and complex machine, does not require high temperature and it is very cheap. Chemical bath deposition of CdS consists of a chemical bath of a salt which contains Cadmium cations and anions of either sulphates, nitrates, chlorides or acetates" [32]. "The properties of CdS thin films obtained by CBD depends on the preparative parameters, hence several studies have been carried out to optimize such parameters such as; bath temperature, pH of bath content, concentration of different precursors and deposition time" [33,34].

This paper reports the dispersion parameters of CdS thin films evaluated from the absorption spectra as a result of variation in deposition time in a chemical bath deposition technique. The accurate determination of these parameters is important not only to know the basic mechanisms but also the underlying phenomena and exploit and develop their interesting technological applications. The dispersion parameters considered are; dispersion energies (E_o, E_d) ,, dielectric constant $(\varepsilon,)$, the average values of oscillator strength (S), wavelength of single oscillator λ, and plasma frequency ω_p. Also considered was the electronic polarizability using

the Lorenz - Lorentz equation and Clausius Mossotti local field model.

2. EXPERIMENTAL DETAILS

CdS thin film was prepared according to our previous work [5] by using ultrasonically cleaned glass substrate of size $(25.0x75.0x1.0)\ mm$. The major precursors for CdS are aqueous solutions from Cadmium acetate for Cadmium source and Thiourea for Sulphide source while Ammonium acetate was used as the complexing agent. All the chemicals used were of analytical grades. The key precursors, Cadmium Acetate ($Cd\ CH_3COO$, Sigma Aldrich, purity 98%) and Thiourea $Sc(NH_2)_2$ Merck, $\geq 98\%$, all were procured through Divine Chemicals Laboratory Ibeagwa Road, Nsukka Nigeria. The bath consists of $30\ ml$ of $0.264gdm^{-3}$ of Cadmium acetate, $15ml\ of\ 0.158gdm^{-3}$ of ammonium hydroxide, $30\ ml\ of\ 0.153gdm^{-3}$ of Thiourea and $20ml\ of\ 1.542gdm^{-3}$ of ammonium acetate which brought the volume of the content of the bath to $95ml$. The temperature of the bath was maintained at 90℃ using 78HW-1 constant magnetic stirrer. The substrates were inserted vertically with the aid of a stand and clips. The deposition was allowed to take place at time intervals of (10, 30, and 50) minutes respectively after which the substrates were removed from the bath simultaneously and rinsed with de-ionized water and then annealed in an oven at a temperature of 400℃ for 60 minutes. we used the gravimetric method in calculating the thickness of the film grown in this work. This method is based on the direct determination of the mass deposited onto the glass substrate. The substrate was weighed before deposition and reweighed after deposition; the thickness was determined using relevant equation. The samples were characterized for optical properties using a single - beam UV-VIS Helios omega spectrophotometer by measuring the absorption of the samples within the wavelength range of $(280-920)\ nm$.

3. RESULTS AND DISCUSSION

3.1 Optical Characterization

Optical measurements of transmittance and absorbance of the films deposited at different deposition times are shown in Figs. 1 and 2. These measurements have been taken in the wavelength range of $(280-920)\ nm$. The transmittance was calculated using equation (2) [35,36].

$$T = \frac{1}{10^A} \quad (1)$$

where A is absorbance as recorded from the spectrophotometer.

From equation (1) it can be understood that

$$A\ \log_{10} T \quad (2)$$

where A is absorbance

The coefficient of absorption (α) was calculated from the absorbance data using Beer Lamberts law [37] which relates the transmittance (T), absorbance (A) and thickness (d) of the film as shown in equation (3a, b)

$$T = e^{\alpha d} \quad (3a)$$

So that

$$\alpha = 2.303\frac{A}{d} \quad (3b)$$

Fig. 1 is the display of the variation of the percentage transmittance with the wavelength λ, from the figure, the deposited thin films showed strong transmittance along the visible range of the spectrum with the transmittance in the order of 10 min > 30 min > 50 min whereas below the absorption edge the transmittance was near zero. It may be that the deposition time have affected the thickness of the film thereby slowing down the speed of the incident wave within the material. The similar phenomenon has been reported in the literature [5,38]. Fig. 2 also is a display of the absorbance spectra which show that the deposited films exhibited strong absorbance and weak transmittance within the wavelength region of $\lambda < 350\ nm$ but above that wavelength there was a good transmittance which is due to excitation and migration of the electrons from the valence band to the conduction band [39].

3.1.1 Optical energy gap

The optical bandgap of CdS was obtained from the Absorbance data using the Tauc's relation [40] as shown in equation (4).

$$(\alpha hv) = A\left(hv - E_g\right)^m \quad (4)$$

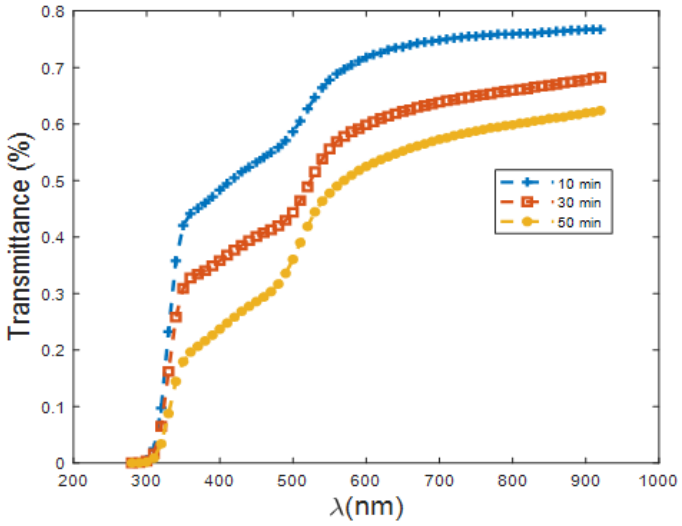

Fig. 1. Variation of Transmittance with the wavelength

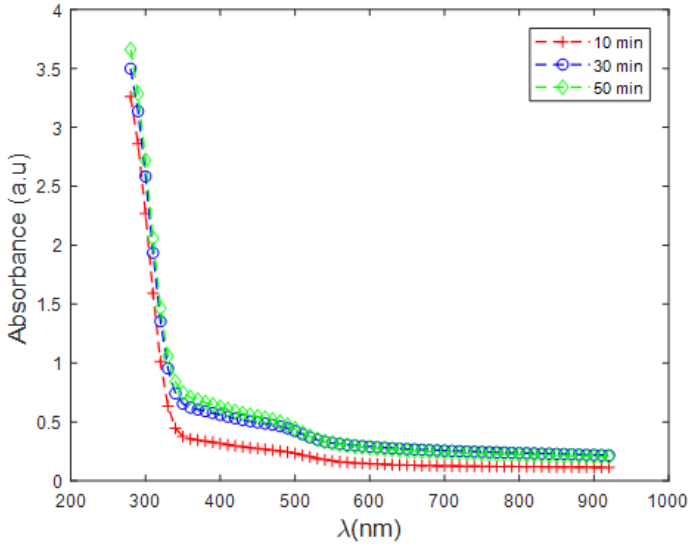

Fig. 2. Variation of absorbance with the wavelength

Where A is a constant called the band tailing parameter, E_g is the bandgap corresponding to a particular transition occurring in the film, ν is the transition frequency, h is the planks constant given by $6.63x10^{-34}m^2kgs^{-1}$, The value of *m* which is the characteristic nature of the band could be $\frac{1}{2}, \frac{3}{2}, 2, \text{or } 3$ depending on the nature of the electronics transition responsible for absorption, $m = \frac{1}{2}$ for direct band gap semiconductors. An extrapolation of the linear region of the plot of $(\alpha h\upsilon)^2$vs $h\upsilon$ gives the value of optical band gap E_g . [41].

Fig. 3 shows the bandgap energy values of the CdS thin films with different deposition times of 10, 30, and 50 minutes and is listed in Table 1. From the result, the bandgap values were found to be higher than that of the bulk material with the film deposited for 10 minutes having higher and that of 50 minutes having the lowest. This condition have been attributed to quantum confinement by some researchers [37,42] The result we obtained is similar to those reported by other researchers [3,37,42,43]. This phenomenon is as a result of the breaking down of the continuum density of state into discrete levels such that bandgap energy widens compared to the bandgap of the bulk [44-46].

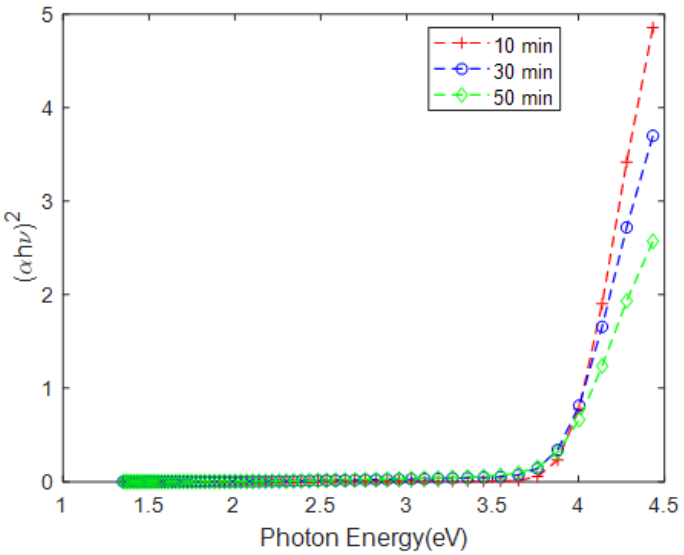

Fig. 3. Plot of $(\alpha h\nu)^2$ vs $(h\nu)$ of CdS thin film of different deposition time

3.1.2 Refractive index analysis

One of the distinctive and essential property of an optical material is its refractive index n.

"This is because it is one of the major factors to be considered in selecting materials used for fabricating optical devices or for optical applications. Therefore, it is essential to understand the refractive index of a material since many optical phenomena are dependent on its value. The refractive index η is closely related to both electronic polarization of ions and the local field inside the optical materials" [47]. The refractive index η was determined using equation (5) [48,49].

$$\eta = \frac{1+\sqrt{R}}{1-\sqrt{R}} \quad 5$$

where R is the reflectance of the film.

The refractive index η of the thin films as a function of photon energy is shown in Fig. 4. From the figure the refractive index peaks near $\sim 2.5eV$ and attains the highest peak at $\sim 3.5eV$ with the thin film that has the lowest deposition time having the highest peak which is an indication that the deposition time influences the refractive index. Many researchers have attributed these peaks to optical transition from valence band to conduction [38]. This shifting of the peaks position is indicative of the change in the optical bandgap of the thin films.

3.1.3 Extinction coefficient

The extinction coefficient k is determined using equation (6) [48,49]

$$K = \frac{\alpha\lambda}{4\pi} \quad 6$$

where α is the absorptioncoefficient and λ is the wavelength of the incident beam.

The extinction coefficient also known as the absorption index is so important in determining several optical measurements that are related to the absorption of light waves in the medium and dielectric constant [50]. "The extinction coefficient k spectra as a function of incident wave is shown in Fig. 5. The figure reveals that the extinction coefficient K decreases with increase in wavelength of the incident photons. At the lower values of K, it should be noted that light energy lost by scattering and absorption per unit distance was having small values when light propagates through the thin films" [50]. Also observed was that the thin film deposited for 30 min have higher K as compared to others which means that there was more scattering of light which may be as a result of impurities or surface morphology. However, the lower values of K at the visible region of the spectrum is an evidence that less light was lost by scattering hence the material is good for optical devices.

The figure shows that the extinction coefficient decreases with increase in the incident waves.

3.1.4 Dielectric constant analysis

"The fundamental electron excitation spectra of CdS thin film are described with complex dielectric constant ε^*. The real part of dielectric

constant ε_r is related with the property of slowing down the speed of light in materials as well as dispersion of electromagnetic waves that travels within the material whereas the imaginary part of the dielectric constant ε_i provides a measure of the disruptive rate of the wave in the material, meaning that it is responsible for the energy absorption from electric field due to dipole motion" [51,52]. The values of real and imaginary part of the dielectric constant were obtained using equation (7 a, & b) [53] and shown in Figs. 6 and 7.

$$\varepsilon_r = \eta^2 - k^2 \quad (7a)$$

and

$$\varepsilon_i = 2\eta k \quad (7b)$$

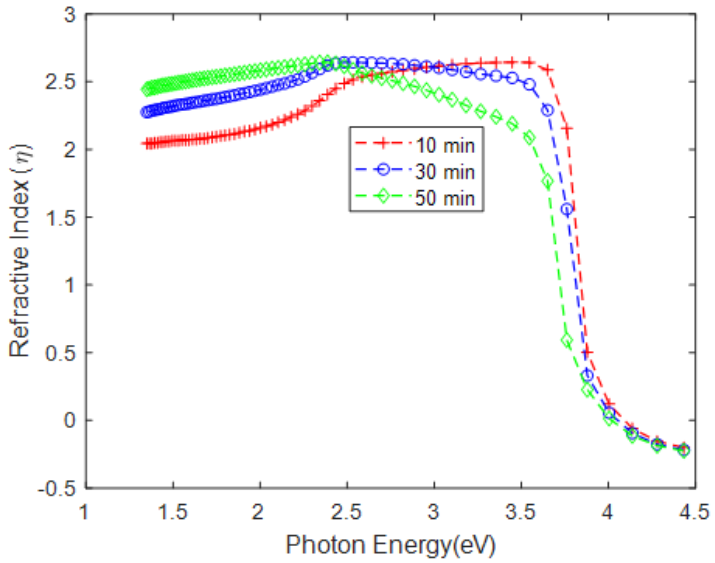

Fig. 4. Plot of $Refractive\ Index\ (\eta)$vs $(h\nu)$ of CdS thin film of different deposition time

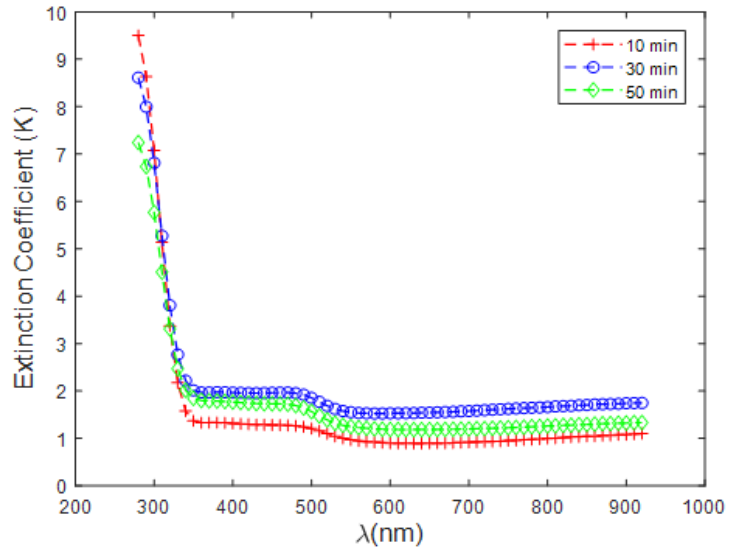

Fig. 5. Plot of $Extinction\ Coefficient\ (K)$ vs $Wavelength\ \lambda(nm)$ of CdS thin film for different deposition time

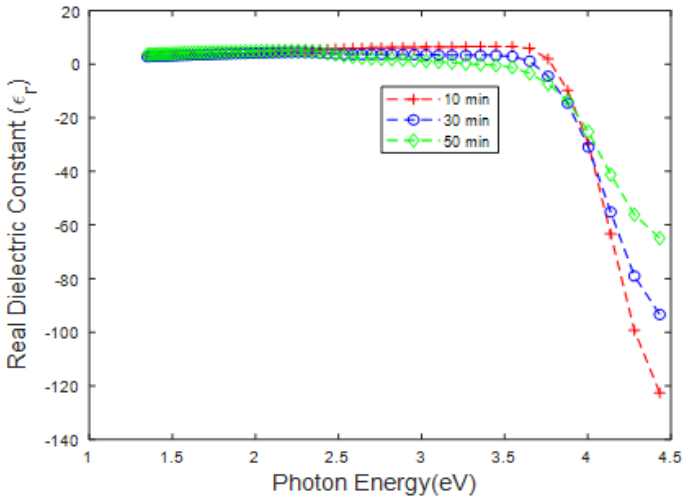

Fig. 6. Plot of $\boldsymbol{Real\ Dielectric\ Constant\ (\varepsilon_r)}$ vs $\boldsymbol{Photon\ energy\ (eV)}$ of CdS thin film of different deposition time

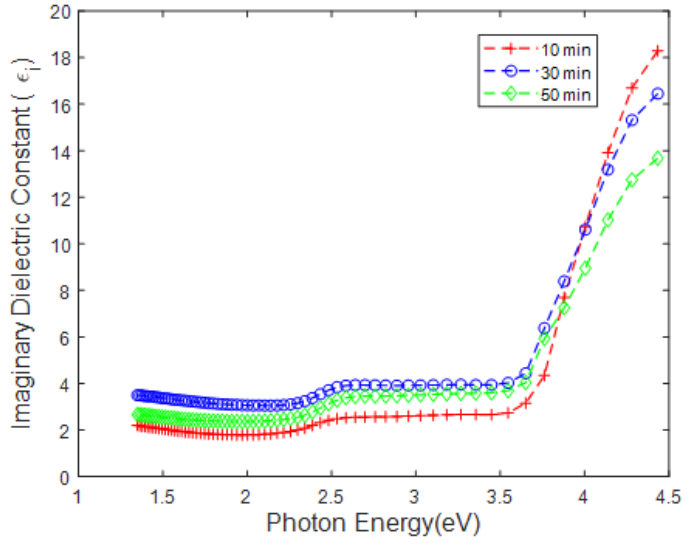

Fig. 7. Plot of $\boldsymbol{Imaginary\ Dielectric\ Constant\ (\varepsilon_i)}$ vs $\boldsymbol{Photon\ energy\ (eV)}$ of CdS thin film of different deposition time

Fig. 6 is a display of the real dielectric constant as a function of photon energy, within the range of $\sim 1.5eV - 2.5eV$, the three films exhibited the same behaviour whereas near the absorption edge as the photon energy is increased there was a gradual shift in the dielectric constant in the order 10 min > 30 min > 50. Fig. 7 also show the imaginary dielectric constant as a function of photon energy which show an exponential increase as the photon energy increase after the absorption edge. This view is in agreement with the assertion of Davis & Mott [50,54].

3.1.5 Dispersion energy parameters

In optical communication and designing devices, the dispersion of the refractive index is very important. The spectral dispersion is obtained from the Wemple DiDomenico model given in equation (8) [55].

$$\eta^2 - 1 = \frac{E_d E_o}{E_o^2 (h\nu)^2} \qquad 8$$

where E_d is dispersion energy and is related to the strength of the inter band optical transition.

E_o is the oscillator energy which gives the quantitative information on the overall band structure of the CdS thin film. By plotting $\frac{1}{n^2-1}$ against the square of the photon energy $(h\nu)^2$ as shown in Fig. 8a. The values of E_d and E_o are calculated from the slope $(E_0E_d)^{-1}$ and intercept $\left({}^{E_0}/_{E_d}\right)$ on the vertical axis as extracted from the linear fit of each of the deposited sample is given in Table 1. From the values of E_d and E_o, the static refractive index (η_o) and static dielectric constant (ε_o) are calculated using equation (9) [55].

The values of E_d and E_o are comparable to the result reported by Wemple and DiDomenico [53]. The Wemple-DiDomenico model have the advantage of providing an intuitive physical interpretation of measured quantities and have been used severally even in ternary chalcogenide systems. This is because it gives information concerning three different energies which are; The average energy gap or the oscillator energy or the effective single oscillator energy E_o of the material which give the overall information of the band structure of the material. Another energy is the dispersion energy E_d which is a measure of the inter-band optical transition and it has to do with the ionicity, anion valency and coordination of the material. The third energy is the incident photon $h\nu$. From the result listed in Table 1, the values of E_o decreases as the deposition time increases and also the values of E_d deposited at 30 min is greater than that deposited at 50 min and 10 min respectively. This could mean that it requires grater energy for inter band optical transitions. The similar phenomenon has been reported in the literature [56,57].

$$\varepsilon_o = {\eta_o}^2 = 1 + \frac{E_d}{E_o} \qquad 9$$

The moments of optical dispersion spectra m_{-1} and m_{-3} are evaluated from equation (10a) and (10b)

$${E_o}^2 = \frac{M_{-1}}{M_{-3}} \qquad 10a$$

And the values of η_o, ε_o, M_{-1} and M_{-3} are listed in Table 1.

$${E_d}^2 = \frac{M_{-1}^3}{M_{-3}} \qquad 10b$$

The values of η_o and ε_o as listed in Table 1 are seen to be increasing as the deposition time is increasing. However, it is noted that at the deposition time of 50 min, the high frequency refractive index (η_∞) is the same as the static refractive index (η_o) and the high frequency dielectric constant (ε_∞) is the same as the static dielectric constant (ε_o) .also from the table the values of M_{-1} and M_{-3} were found to be increasing as the deposition time. Our result can be compared to the result reported by Ikhmayies [58].

The Wemple–Didomenico formula can be modified to find the static optical index of refraction at infinite wavelength [58-60] in the form of

$$\frac{\eta_\infty^2-1}{\eta^2-1} = 1 - \left(\frac{\lambda_0}{\lambda}\right)^2 \qquad 11a$$

By plotting $\frac{1}{n^2-1}$ against λ^{-2} of CdS as shown in Fig. 8b, the high frequency refractive index (η_∞) was calculated from the intercept extracted from the linear fit of each of the deposited sample whereas $\eta_\infty^2 = \varepsilon_\infty$ and were also listed in Table 1.

Using the single Sellmeier oscillator model, [50] equation (11b), the oscillator strength and oscillator wavelength of CdS thin film were evaluated and listed in Table 1.

$$\eta^2 - 1 = \frac{S_o\lambda_o^2}{1-\left(\frac{\lambda_o}{\lambda}\right)^2} \qquad 11b$$

Where λ is incident wavelength, S_0 is oscillator strength and λ_0 is oscillator wavelength. By plotting $\frac{1}{n^2-1}$ against λ^{-2} of CdS as shown in Fig. 8b. The values of S_o and λ_o are obtained from the slope and intercept extracted from the linear plot of all the deposited samples and are listed in Table 1, which show that S_o value for film deposited for 30 min is greater than S_o value for films deposited for 10 min and 50 min respectively while λ_o increases with increase in deposition time.The lattice dielectric constant (ε_L) of CdS thin film is also calculated from equation (12) [61].

Table 1. Optical and dispersion parameters of CdS thin films

Time	10 min	30 min	50 min
E_g	3.78 eV	3.72 eV	3.70 eV
E_d	13.16 eV	27.64 eV	20.98 eV
E_o	4.44 eV	4.25 eV	1.48 eV
η_o	1.99	2.75	3.90
ε_o	3.96	7.58	15.18
M_{-1}	2.96	6.50	14.18
M_{-3}	0.1502 eV^2	0.36 eV^2	6.47 eV^2
S_0	3.795×10^{-5}	7.62×10^{-5}	2.02×10^{-5}
λ_o	279.30 nm	292.22 nm	838.50 nm
η_∞	1.72	2.74	3.90
ε_∞	2.96	7.51	15.18
ε_L	7.02	5.99	5.30
$\frac{N}{M^*}$	$1.62 \times 10^{41} kg^{-1}m^{-3}$	$2.31 \times 10^{41} kg^{-1}m^{-3}$	$5.8 \times 10^{41} kg^{-1}m^{-3}$
ω_p	$1.25 \times 10^6 Hz$	$8.18 \times 10^5 Hz$	$1.30 \times 10^6 Hz$
α_p	$9.27 \times 10^{-33} Fm^2$	$7.90 \times 10^{-33} Fm^2$	$1.01 \times 10^{-33} Fm^2$

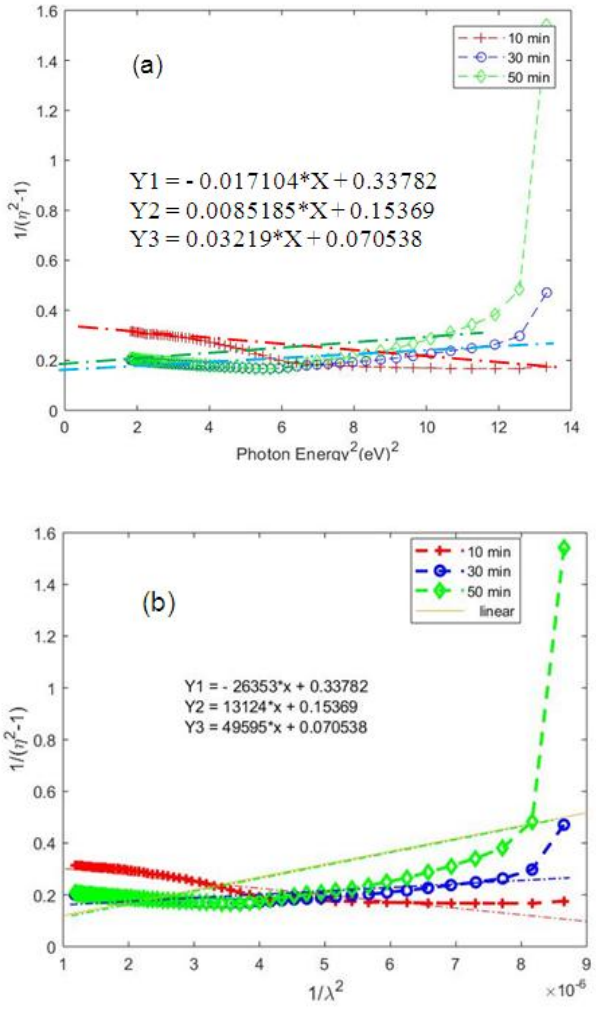

Fig. 8. (a) $\frac{1}{\eta^2-1}$ $Versus$ $h\nu^2$ (b) $\frac{1}{\eta^2-1}$ $Versus$ $\frac{1}{\lambda^2}$

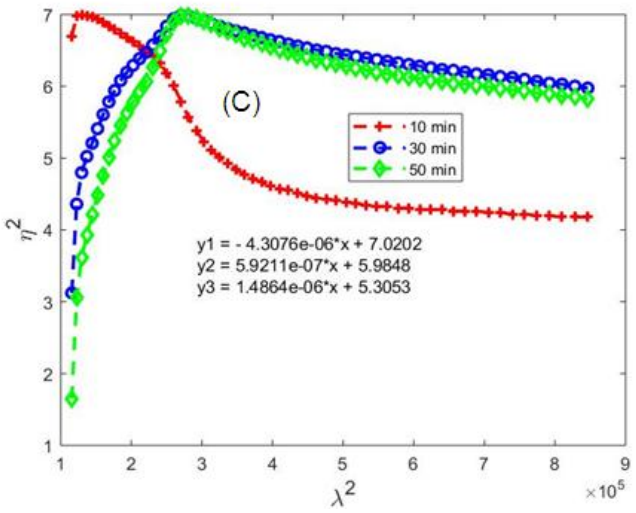

Fig. 8(c) η^2 *Versus* λ^2

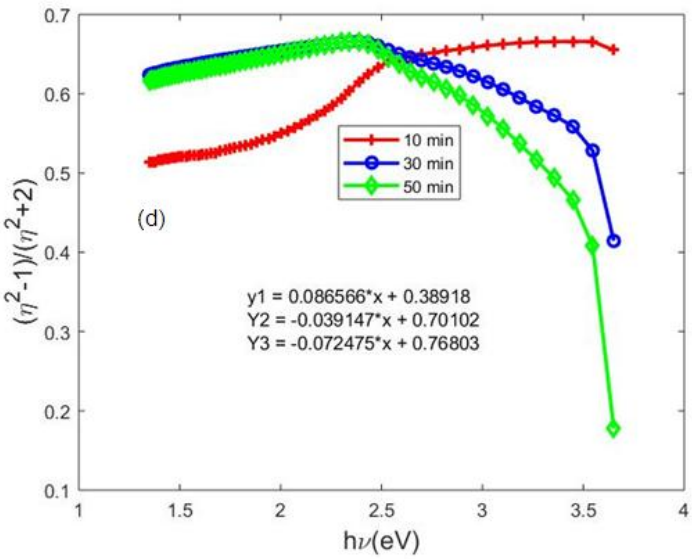

Fig. 8(d). $\frac{\eta^2-1}{\eta^2+2}$ *Versus* $h\nu$ (eV)

$$\eta^2 = \varepsilon_L - \left[\frac{e^2}{4\pi c^2 \varepsilon_o}\frac{N}{M^*}\right]\lambda^2 \quad (12)$$

where e is the charge of electron, c is the speed of light, ε_0 is the permittivity of free space, $\frac{N}{M^*}$ is the ratio of number of free charge carriers and effective mass of electrons. Also, the plasma resonance frequency ω_p which is referred to as the material change from metallic to dielectric can be evaluated from the curve n^2 versus λ^2 using equation (13) [50].

$$\eta^2 = \varepsilon_L - \left(\frac{\omega_p^2}{4\pi c^2}\right)\lambda^2 \quad (13)$$

Using Fig. 8c, the values of ε_L, $\frac{N}{M^*}$ and ω_p were obtained and listed also in Table 1. The lattice energy ε_L gives information about the strength of the bonds in ionic compound. This is a potential that acts on the electrons, restoring it to its mean position when incident's light electric field sends it into oscillation. As is observed from the table, the lattice energy of the deposited thin film increases as the deposition time increases.

3.1.6 Electronic polarizability

"The electronic polarizability (α_p) gives the degree of the electronic response to the

application of an electromagnetic field on the electron clouds" [56]. The polarizability (α_p) of CdS thin film can be evaluated using Lorenz - Lorentz equation and Clausius Mossotti local field model [61,62] as shown in equation (14).

$$\left(\frac{\eta^2-1}{\eta^2+2}\right) = \frac{N_A\rho}{3\varepsilon_o M}\alpha_p \qquad 14$$

where η is the refractive index, N_A is the Avogadro's number M is the molar mass of bulk CdS and ρ is the density of bulk CdS. Therefore, the plot of $\frac{n^2-1}{n^2+2}$ against $h\nu$ of CdS thin film is shown in Fig. 8(d). The intercept of plot on the vertical ais gives the value of α_p and listed in Table 1, as extracted from the linear plot of the deposited samples. From Fig. 8d it is observed that within $\sim 2.5eV$ all the deposited thin films have the same response to the application of photon energy, but as the photon energy increases, the electronic response changes with the thin film deposited for 10 min having the highest response.

4. CONCLUSION

Cadmium Sulphide (CdS) thin film was deposited by chemical bath deposition technique on a transparent glass substrate. The CdS thin film has a very high transmittance through the entire electromagnetic spectral range which justify it as a good material for optoelectronic devices and solar cells. The dielectric constant was evaluated from the linear refractive index and extinction coefficient. The dispersion parameters $(E_d,\ E_0, moment\ of\ optical\ spectra\ S_0\ ,\ \lambda_0\ ,\ \frac{N}{M^*}\ ,\ \omega_p,$ and $\alpha_p,)$ dielectric constants $(\eta_0, \eta_\infty, and\ E_L)$ have been evaluated using Wemple DiDomenico model and single Sellmeier oscillator model. The electronic polarizability of CdS thin film was evaluated using Clausius - Mossotti local field polarizability model.

ACKNOWLEDGEMENT

The authors are thankful to the Department of Physics, University of Abuja for the support and also the Advanced Physics Laboratory, Sheda Science and Technology complex (SHETSCO) Abuja for allowing us to use their laboratory facilities in carrying out this research.

COMPETING INTERESTS

Authors have declared that no competing interests exist.

REFERENCES

1. Suresh Babu K, Vijayan C, Haridoss P. Synthesis of size-tunable and stable CdS nanocrystals in DMF. Materials Letters. 2006;60(1):124-8.
2. Okorie O, Buba ADA, Ramalan AM. Optical and dielectric properties of cadmium sulphide thin film grown using chemical bath deposition technique. IOSR JAP (IOSR-JAP). 2017;9(5):82-9.
3. Nwofe PA, Agbo PE. Effect of deposition time on the optical properties of cadmium sulphide thin films. Int J Thin.Fil. Sci. Tec. 2005;4(2):63-7.
4. Akl AA, Hassanien AS. Microstructure and crystal imperfections of nanosized CdSxSe1-x thermally evaporated thin films. Superlattices Microstruct. 2015; 85:67-81.
5. Okorie O, Buba ADA, Ramalan AM. Influence of thickness on the optical properties of cadmium sulphide Thin Film deposited by chemical bath deposition technique. Phys Sci Int J. 2017;16(1):1-11. Article no. PSIJ.35738 ISSN: 2348-0130.
6. Khan ZR, Zulfequar M, Khan MS. Optical and structural properties of thermally evaporated cadmium sulphide thin films on silicon [1 0 0] wafers. Mater Sci Eng B. 2010;174(1-3):145-9.
7. Mahmoud SA, Alshomer S, Tarawnh MA. Structural and optical dispersion characterization of sprayed nickel oxide thin films. J Mod Phys. 2011;2:1178-86.
8. Pan A, Yang H, Yu R, Zou B. Fabrication and photoluminescence of high-quality ternary CdSSe nanowires and nanoribbons. Nanotechnology. 2006;17(4): 1083-6.
9. Yadav AA, Barote MA, Chavan TV, Masumdar EU. Influence of indium doping on the properties of spray deposited CdS0.2Se0.8 thin films. Journal of Alloys and Compounds CdS0. 2011;509(3):916-21.
10. Dhatchinamurthy L, Thirumoorthy P, Arunraja L, Karthikeyan S. Synthesis and characterization of cadmium sulfide (CdS) thin film for solar cell applications grown by dip coating method. Mater Today Proc. 2020;26:3595-9.
11. Ojeda-Barrero G, Oliva-Avilés AI, Oliva AI, Maldonado RD, Acosta M, Alonzo-Medina GM. Effect of the substrate temperature on the physical properties of sprayed-CdS films by using an automatized perfume

atomizer. Mater Sci Semicond Process. 2018;79:7-13.

12. Thambidurai M, Muthukumarasamy N, Murugan N, Agilan S, Vasantha S, Balasundaraprabhu R. Development of mathematical model for prediction and optimization of particle size in nanocrystalline CdS thin films prepared by sol-gel spin- coating method. Metal Mater Trans B. 2010;41(6):1338-45.
13. Mousavi SH, Jilavi MH, Müller TS, de Oliveira PW. Formation and properties of cadmium sulfide buffer layer for CIGS solar cells grown using hot plate bath deposition. J Mater Sci Mater Electron. 2014; 25(6):2786-94.
14. Esmaeili-Zare M, Behpour M. Fabrication and study of optical properties on CdS semiconductor as buffer layer for Cu(In,Ga)Se2 thin film solar cells. J Mater Sci Mater Electron. 2017;28(14):10173-83.
15. Jun-feng H, Gan-hua F, Krishnakumar V, Cheng L, Jaegermann W. CdS annealing treatments in various atmospheres and effects on performances of CdTe/CdS solar cells. J Mater Sci Mater Electron. 2013;24(8):2695-700
16. Sami R, Ghazai AJ. Preparation and characterization of structural and optical properties of CdS thin film spin coating prepared. J Phys Conf Ser 1999012070. 2021;1999(1).
17. Aliyu M, Diso DG, Musa AO, Abubakar AI. Effect of growth voltage on electrodeposited CdS thin films. Bayero J Pure Appl Sci. 2022;13:539-45.
18. Shanmugapriya S, Sakthivel B, Nandhabalaji S. ZnSe/CdS thin films prepared with physical vapour deposition technique. Adalya J. 2020;9:635-40.
19. Shaikh SS, Shkir M, Masumdar EU. Facile fabrication and characterization of modified spray deposited cadmium sulphide thin films. Phys B. 2019;571:64-70.
20. Gopalakrishnan P, Amalraj L, Vijayakumar K. Deposition and characterization of spray pyrolytic cadmium sulphide thin film [film]. Int J Thin.Film. Sci Tec. 2023;12(1):9-12.
21. Hamad NH, Faraj MG. Structural and optical properties of cadmium sulfide-doped silver deposited on glass and polymer substrates by chemical spray pyrolysis. Aro-the Scientific Journal of Koya University. 2023;11(1):32-7.
22. Holi AM, Al-Zahrani AA, Najm AS, Chelvanathan P, Amin N. PbS/CdS/ZnO nanowire arrays: synthesis, structural, optical, electrical, and photoelectron-chemical properties. Chem Phys Lett. 2020;750:137486.
23. Najm AS, Chowdhury MS, Munna FT, Chelvanathan P, Selvanathan V, Aminuzzaman M et al. Impact of cadmium salt concentration on cds nanoparticles synthesized by chemical precipitation method. Chalcogenide Lett. 2020;17(11): 537-47.
24. Mohamed S, Mona M, Hany H. Morphological and optical study of sol-gel spin coated nanostructure CdS thin films. Int. Org. Sci Res. 2015;7;19-22:(6-1).
25. Sharma B, Lalwani R, Das R. Spectroscopic studies of CdS Nanocrystalline thin films synthesized by sol-gel spin coating technique for optoelectronic application: influence of co-doping. Braz J Phys. 2023;53(2):42.
26. Ziaul RK, Zulfequar M, Khan MS. Effect of thickness on structural and optical properties of thermally evaporated cadmium sulfide polycrystalline thin Films. Chalcogenide Lett. 2010;7(6):431-8.
27. Nafiseh M, Seyeed MR, Isabella C, Alberto V. Deposition of nanostructure CdS thin films by thermal evaporation method: Effect of substrate temperature. J Mater Sci. 2017;10:773-80.
28. Alam A, Kumar S, Singh DK. Cadmium sulphide thin films deposition and characterization for device applications. Mater Today Proc. 2022;62:6102-6.
29. Najm AS, Naeem HS, Alwarid DARM, Aljuhani A, Hasbullah SA, Hasan HA; et al. Mechanism of chemical bath deposition of CdS thin films: influence of sulphur precursor concentration on microstructural and optoelectronic characterizations. Coatings. 2022;12(10):1400.
30. Toma FTZ, Hussain KMA, Rahman MS, Ahmed S. Preparation and characterization of CdS thin film using chemical bath deposition (CBD) technique for solar cell application. World J Adv Res Rev. 2021; 12(3):629-33.
31. Tsuchikado H, Chen M, Guan G, Abe T. Efficient photoanode characteristics of cadmium sulfide films multi-deposited through a chemical bath deposition process. J Appl Electrochem. 2023.
32. Martinez JL, Martinez G, Torres-Delgado G, Guzman O, Del Angel P, Lozada-Morales R. Cubic CdS thin films studied by spectroscopic ellipsometry. J Mater Sci Mater Electron. 1997;8(6):399-403.

33. Sengupta S, Aggarwal R, Raula M. A review on chemical bath deposition of metal chalcogenide thin films for heterojunction solar cells. J Mater Res. 2023;38(1):142-53.
34. Narayana Swamy TN, Pushpalatha HL, Ganesha R. Chemically deposited CdS thin film and its photoelectric performance. J Chem Biogr Physiol Sci Sec C. 2017; 7(1):119-30.
35. Lothian GF. Absorption spectrophotometer. 2nd ed" Hisher and Watts Ltd London. 1958;19-20.
36. Pankove JI. Optical processes in semiconductors. Prentice – hall New York; 1971.
37. Ruby D, Suman P. Comparison of Optical Properties of Bulk and nanocrystalline Thin Films of CdS using different Percursors. Int J Mat Sci. 2011;1:35-40.
38. Yakuphanoglu F, Viswanathan C, Peranantham P, Soundarrajan D. Effects of the film thickness on optical constants of transparent CdS thin films deposited by chemical bath Deposition. J Optoelectron Adv Mater. 2009;11:945-9.
39. Kumar C, Donoso B, Silva H, Padilla-Campos L, Zarate A. The enhanced light trapping nature of NiOx thin films deposited by magnetron sputtering onto silicon solar cells at room temperature. Mater Lett. 2021;297:129961.
40. Usha KS, Sivakumar R, Sanjeeviraja C. Optical constant and dispersion energy of NiO thin films prepared by radio frequency magneto sputtering technique. J Appl Phys. 2013;114(12):123501-10.
41. Sharma AK, Vishwakarma AK, Yadava L. Optical and structural properties of CdS-ZnO thick film. Mater Lett X. 2023;17:100180, ISSN 2590-1508.
42. 42, Tizazu A, Francis KA, Fekadu GH, Isaac N, Robert KN, Francis B. A new route for the synthesis of CdS thin films from acidic chemical baths. Int J Thin Fil Sci Tec. 2017;6(2):67-71.
43. Sahraei R, Shahriyar S, Majles-Ara MH, Daneshfar A, Shokri N. Preparation of nanocrystallineCdS thin films by a new chemical bath deposition route for application in solar cells as antireflection coatings. Prog. Color colorants Coat. 2010; 3:82-90.
44. Thambidurai M, Murugan N, Muthukumarasamy N, Vasantha S, Balasundaraprabhu R, Agilan S. Preparation and characterization of nanocrystalline CdS thin films. Chalcogenide Lett. 2009;6(4):171-9.
45. Oliva AI, Solıs-Canto O, Castro-Rodriguez R, Quintana P. Formation of the band gap energy on CdS thin films growth by two different techniques. Thin Solid Films. 2001;391(1):28-35.
46. Mir FA, Chattarjee I, Dar AA, Asokan K, Bhat GM. Preparation and characterization of cadmium sulfide nanoparticles. Optik. 2015;126(11-12):1240-4.
47. You ZZ, Hua GJ. Electrical, Optical and microstructure properties of transparent conducting GZO thin films deposited by magnetron sputtering. J Alloys Compd. 2012;530:11-7.
48. Aziz MS, El-Mallah HM. Electrical and Optical Properties of azo dye. Indian J Pure Appl Phys. 2009;47:530-4.
49. Desai HN, Dhimmar JM, Modi BP. Study of linear and non-linear optical parameters of zinc selenide thin film int. J Eng Res Appl ISSN: 2248-9622. 2015;5(6): 117-22.
50. Hassanien AS. Studies on dielectric properties, opto-electrical parameters and electronic polarizability of thermally evaporated amorphous Cd50S50-xSex thin films. J Alloys Compd. 2016;671: 566-78.
51. Sharma P, Sharma V, Katyal SC. Variation of optical constant in Ge10Se60Te30 thin film. Chalcogenide Lett. 2006;3:73-9.
52. Wooten F. Optical properties of solids, academic press New York London; 1972.
53. Wemple SH, DiDomenico M. Behavior of the electronic dielectric constant in covalent and ionic materials. Phys Rev B. 1971;3(4):1338-51.
54. Davis EA, Mott NF. Conduction in non-crystalline system V. Conductivity, optical absorption and photoconductivity in amorphous semiconductors. Philos Mag. 1970;22(179):903-22.
55. Ahmad AA, Alsaad AM, Albiss BA. Al−Akhras, M-Ali, El-Nasser HM, Qattan. The Eff substrate temp struct opt prop of D.C. sputtered ZnO thin films. Physica B: Condensed Matter. I.A:470-1:21–32.
56. Hassanien AS, Akl AA. Influence of composition on optical and dispersion parameters of thermally evaporated non-crystalline Cd50S50_xSex thin films. J Alloys Compd. 2015;648:280-90.
57. Yakuphanoglu F, Cukurovali A, Yilmaz İ. Determination and analysis of the

dispersive optical constants of some organic thin films. Phys B. 2004;351(1-2):53-8.

58. Ikhmayies SJ. A study of the optical parameters of cds thin films prepared by thermal evaporation. J Amasya Univ Inst Sci Technol. 1(1): 56-73.
59. Yeh P, Hendry M. Optical waves in layered media. Phys Today. 1990;43(1): 77-8.
60. Moss TS, Burell GJ, Ellis E. Semiconductor optoelectronic, (Butterworths, London, 1973).
61. El-Morsy MAM, Wahba HH. Determination of the optical Properties of a bent Optical Fiber by Using an automatic Fringe Pattern Analysis. J Korean Phys Soc. 2011;59(5): 3080-8.
62. Olson JD. The refractive index and Lorenz–Lorentz function of fluid methane. J Chem Phys. 1975;63(1):474-84.

Peer-review history:
The peer review history for this paper can be accessed here:
https://www.sdiarticle5.com/review-history/98416